Research Square

Preprints are preliminary reports that have not undergone peer review.
They should not be considered conclusive, used to inform clinical practice,
or referenced by the media as validated information.

Spatio-temporal Variations of Zn, Cu, Cd, Pb, Se, and Sn in Sediments Around a Kappaphycus Seaweed Farm and Its Associated Risks

Reyland Alegroso

raalegroso@up.edu.ph

University of the Philippines Visayas

Nathaniel Añasco

University of the Philippines Visayas

Mae Grace Nillos

University of the Philippines Visayas

Sheila Mae Santander-de Leon

University of the Philippines Visayas

Kazuki Imamura

Kagoshima University

Emiko Kokushi

Kagoshima University

Seiichi Uno

Kagoshima University

Research Article

Keywords: metal pollution, Kappaphycus seaweed farm, selenium, sediments

Posted Date: March 31st, 2026

DOI: https://doi.org/10.21203/rs.3.rs-9111716/v1

License: This work is licensed under a Creative Commons Attribution 4.0 International License. Read Full License

Additional Declarations: Competing interest reported. This work was supported by the UPV OVCRE Student's Theses Support Grant, project number SP24-12, and by the UP OIL COOPERATE Mobility Grant, grant number OILCOOP-2024-15. The funders had no role in study design, data collection, data analysis, interpretation, writing, or decisions regarding publication. The authors declare no other competing interests.

Abstract

Coastal development and maritime activities continue to introduce metals into nearshore environments, including seaweed farms. Despite the rapid expansion of tropical seaweed aquaculture, sediment metal, naturally and anthropogenic in origin, dynamics within active *Kappaphycus* farming areas remain poorly characterized, particularly with respect to the bioavailable metal fraction that controls ecological exposure. This study quantified bioavailable Zn, Cu, Cd, Pb, Se, and Sn in sediments surrounding a *Kappaphycus* farm in Concepcion, Iloilo, Philippines, from September to November 2024 and evaluated their associated risks. Sediments showed low bioavailable concentrations, with 2.26 to 13.1 mg kg^{-1} Zn, 0.258 to 2.22 mg kg^{-1} Cu, 0.0455 to 0.0718 mg kg^{-1} Cd, 0.268 to 3.00 mg kg^{-1} Pb, and 1.12 to 4.61 mg kg^{-1} Sn, but considerably high Se of about 3.32 to 14.3 mg kg^{-1}. Spatial patterns showed higher metal concentrations in fine grained sediments with higher moisture content and organic matter. Temporal observations during the cultivation period indicated declining metal concentrations. Most metals in sediments were below commonly used guideline thresholds, suggestive of low potential ecological concern, except for Se, which warrants attention due to trophic relevance. These findings show low ecological risk from most metals under present conditions, while elevated selenium concentrations warrant continued monitoring due to its known bioaccumulative behavior. The study provides information on bioavailable metals in sediments of tropical seaweed farms and demonstrates the influence of sediment characteristics on metal distribution within mariculture environments.

Introduction

Coastal ecosystems next to rapidly expanding rural and semi-urbanized areas are subjected to varied combinations of pollutants from stormwater runoff, atmospheric deposition, household wastewater, industrial operations, and intensive agriculture (Shimod et al., 2022). These inputs accumulate in nearshore waters, where limited circulation and sedimentation facilitate the retention of trace metals (El-Sharkawy et al., 2025). Impenetrable urban surfaces increase pollutant movement by lowering natural infiltration, while insufficient wastewater treatment facilities elevate metal discharge into rivers, estuaries, and shallow aquaculture areas (Shimod et al., 2022). Several tropical coastal farming systems now function within chemically modified environments influenced by both diffused and point sources.

Seaweeds occupy a central position in these coastal systems. *Kappaphycus* species are rapidly proliferating tropical macroalgae extensively grown for carrageenan, with major production in the Philippines (Mateo et al., 2021). The biology of *Kappaphycus*, its rapid vegetative growth, and the extensive development of mariculture allow for cultivation in shallow, sediment-influenced waters (Ask et al., 2003). These characteristics assist their role as bioindicators and raise concerns over food safety, since grown macroalgae may acquire contaminants from sediments and surrounding environment (Rubio et al., 2010). In the Philippines, seaweed farming has considerable economic advantages. In 2022, seaweed production reached 1.54 million metric tons, accounting for 35.6% of the overall fisheries output (PSA, 2023). These farms are often situated in nearshore waterways and are affected by rivers in some areas, urban effluents, and sediment transport (Mateo et al., 2021). This spatial overlap establishes exposure paths for metals.

Trace metals persist in sediments, accumulate in biota, and may pose ecological and human health risks. Zinc (Zn) and copper (Cu) are essential micronutrients that support enzymatic and metabolic functions but induce physiological stress at elevated concentrations (Besada et al., 2009). Cadmium (Cd) and lead (Pb) have no known biological role and are toxic even at low concentrations, raising concern for benthic organisms and seafood consumers (Besada et al., 2009). Selenium (Se) contamination is known to be associated with coal related activities

(Lemly, 2009) and has tendency to transfer efficiently through the sediment to biota pathway, rather than through direct sediment toxicity alone (Janz et al., 2010). Inorganic tin (Sn) serves as an indicator of industrial inputs and may act as a precursor for the formation of organotin compounds (Langston et al., 2020). Previous studies in the Philippines have documented widespread contamination of Zn, Cu, Cd, and Pb in mining affected and urban coastal systems and have identified sediments as long term reservoirs and secondary sources of these metals to biota (Siddique et al., 2025). In contrast, selenium and inorganic tin remain poorly characterized in local coastal sediments, particularly within active seaweed farming areas, providing additional justification for their assessment in this study.

Sediments act as the primary repository for metals, with retention controlled by grain size, redox conditions, and organic matter content. Metals may be remobilized during pH changes, dredging activities, or storm events, increasing their availability to benthic organisms (El-Sharkawy et al., 2025). Sediment quality guidelines and contamination indices, including the contamination factor (CF), geoaccumulation index (I_{geo}), and pollution load index (PLI), are widely used to contextualize metal concentrations (Long et al., 1995; MacDonald et al., 2000; Hakanson, 1980; Müller, 1969; Tomlinson et al., 1980). In the Philippines, these tools have been applied mainly in mining impacted rivers, industrial estuaries, and urban bays (Gangoso et al., 2022).

Despite the rapid expansion of tropical seaweed farming, sediment metal dynamics within active farming environments remain poorly documented. Most previous studies in the Philippines have examined metal contamination in mining-affected rivers, industrial estuaries, or urban bays (Siddique et al., 2025), while aquaculture sediments have received limited attention. This limitation becomes more critical given that ecological risk in seaweed farming areas depends not only on total metal concentrations but on the fraction that seaweeds can absorb. Existing monitoring programs also commonly rely on single-time-point sampling and focus on total metal concentrations, which may obscure short-term variations in bioavailable metals during cultivation cycles. This lack of information limits understanding of potential metal exposure pathways within seaweed farms and their implications for aquaculture sustainability and environmental monitoring. Metal bioavailability represents the fraction of metals that can be absorbed by organisms and therefore provides a more direct indicator of ecological exposure than total sediment concentrations (Barik et al., 2022). Previous studies have shown that elevated bioavailable fractions are associated with increased metal uptake by benthic organisms and potential sublethal physiological effects (Cyriac et al., 2021). As a result, assessing bioavailable metals is critical for evaluating ecological risks in dynamic coastal systems such as seaweed farming areas (Pereira et al., 2023).

This study quantified bioavailable Zn, Cu, Cd, Pb, Se, and Sn in sediments surrounding an active *Kappaphycus* seaweed farm in Concepcion, Iloilo, Philippines, over a three-month cultivation cycle from September to November 2024. The study examined spatial distribution of metals across farm and non-farm sites, evaluated temporal variation within the cultivation period, and assessed relationships between bioavailable metals and sediment characteristics including grain size, moisture content, redox potential, and total organic matter. Sediment quality guideline frameworks and indices were applied to evaluate pollution level and potential ecological risks associated with measured concentrations. This approach provides a regional assessment of bioavailable metals within a tropical seaweed farming environment and establishes information relevant to environmental monitoring and aquaculture management.

Materials and Methods

Sampling area and sample collection

The seaweed farm is located in Concepcion, Iloilo, Philippines (11.219656 N, 123.125901 E; Fig. 1) and is situated within a coastal area influenced by multiple anthropogenic activities. A coal fueled power generation facility operates in the adjacent area. This plant receives coal monthly via cargo vessels and generates 135 MW of electricity, supplying about one third of Panay Island's power demand. Vessel traffic occasionally passes near the farm, and nearby areas host mariculture activities. These activities represent potential point and nonpoint sources of trace metals to the surrounding coastal environment. The sampling sites are shown in Fig. 1, which was generated from Google Earth using QGIS 3.34. The sampling sites, near a coal-fueled power plant, coastal residential area, and municipal docking and fishing port (Table S1), traversed the mainland of Concepcion, Iloilo, Philippines, from Barangay Nipa (Station 1) to Barangay Poblacion (Stations 8–10; emphasized with white-colored box shape), for about 2,832 m in length. The *Kappaphycus* farm (emphasized with a white-colored box shape) was in Sitio Punta Luiz, Barangay Poblacion, Concepcion, Iloilo, Philippines, at 11.219656 N and 123.125901 E, with an area of about 700 m². Ten sampling points were established, three inside and seven outside the farm. Station 1 faced the power plant, while the remaining stations were laid out by triangulation toward the farm interior and toward residential areas, mariculture zones, and boat routes (Table S1) to capture potential coastal inputs and spatial gradients. Sediments from outside the farm were collected in September 2024 for spatial distribution analysis. Sediment samples inside the farm were taken in September, October, and November 2024 to cover the period from planting to the expected harvest. Samples were stored in thermoregulated or Styrofoam boxes with ice and immediately transported to the laboratory.

Surface sediment samples were collected from the upper 2 cm layer beneath the seaweed farm and at stations outside the farm. At each station, about 400 g of sediment were collected using a syringe (internal diameter: 3.10 cm) corer for direct surface sampling. In areas not accessible by hand, an Ekman grab was first deployed to collect bulk sediment. Sub-samples of the upper 2 cm layer were collected using the syringe corer (n = 3). In the laboratory, sediments were air-dried at room temperature for about 14 days, sieved through a 1 mm non-metal (Nytex) plastic sieve, homogenized, and stored in Ziplock bags at room temperature or below until analysis.

Sediment characterization

Sediment properties were assessed through measurements of redox potential, grain size, moisture content, and total organic matter. Redox potential followed Naciongayo and Santander de Leon (2024) using a redox meter (Horiba) with an Ag/AgCl probe inserted into the upper 1 cm of sediment. Grain size, moisture content, and total organic matter followed Holme and McIntyre (1971). In grain sizing, 25 g of sediment were oven-dried at 105°C for 24 h, cooled in a desiccator, and dry-sieved for 15 mins. Grain size classes followed the Wentworth Scale, reporting fractions of very coarse sand (> 1000 μm), coarse sand (1000 to 500 μm), medium sand (500 to 250 μm), fine sand (250 to 125 μm), very fine sand (125 to 62 μm), and silt/clay (< 62 μm). Moisture content used the same dried subsamples by taking the difference between initial (wet weight) and final weights (dry weight) and dividing by the final weight, then multiplying by 100. To determine total organic matter through loss of ignition, 40 g of sediment were oven-dried at 80°C for 24 hours, cooled in a desiccator, and weighed before igniting three 10 g subsamples in pre-weighed crucibles at 550°C for 4 hours; these subsamples were then reweighed after cooling to a constant mass to estimate the loss on ignition. All measurements were done in triplicate and expressed as percentages when applicable.

Chemicals and reagents

All chemicals and reagents used in the experiments were of analytical-grade quality. These include nitric acid (Wako Pure Chemical, Japan), hydrochloric acid (Wako Pure Chemical), perchloric acid (Kishida Chemical, Japan), EDTA (Tokyo Chemical Industry, Japan), hydroxylamine hydrochloride (Wako Pure Chemical), methyl orange (Wako Pure Chemical), ammonium hydroxide (Wako Pure Chemical), diaminonaphthalene (Tokyo Chemical Industry), cyclohexane (Wako Pure Chemical), Cd standard solution (Cd 1000; Wako Pure Chemical), Cu standard solution (Cu 1000; Wako Pure Chemical), Pb standard solution (Pb 1000; Wako Pure Chemical), Zn standard solution (Zn 1000; Wako Pure Chemical), Se standard solution (Se 1000; Wako Pure Chemical), and Sn standard solution (Sn 1000; Wako Pure Chemical). Ultrapure (milli-Q) and deionized water were used throughout all experiments. All glassware and containers were cleaned with phosphate-free soap (Contaminon®, Wako Pure Chemical), soaked for 48 hours in 10% (v/v) HNO_3 and then thoroughly rinsed with ultrapure and deionized water.

Extraction of Zn, Cu, Cd, Pb, and Sn in sediments

Bioavailable metals in sediments were extracted by cold digestion following Uno et al. (2017). Five grams of air-dried sediment were placed in 50 mL polypropylene tubes and mixed with 30 mL of 1 M HCl. Tubes were capped and briefly loosened to release initial gas. Samples were shaken for 2 h at room temperature at 120 strokes per minute and allowed to settle for 30 mins, then vented again. The mixtures were centrifuged at 2000 rpm for 10 mins at 4°C to obtain the supernatant. The supernatant was filtered through a glass filter fitted with a Whatman (47 mm) microfiber filter and transferred to clean polypropylene tubes. Filtrates were capped, wrapped in aluminum foil, stored, and analyzed by FAAS.

Measurement of each metal

Polarized Zeeman Flame Atomic Absorption Spectrophotometer (Hitachi Z-2000, Japan) was used to quantify Zn, Cu, Cd, Pb, and Sn. The analytical wavelengths applied were 213.9 nm for Zn, 324.8 nm for Cu, 228.8 nm for Cd, 283.3 nm for Pb, and 224.6 nm for Sn. The instrumental operating conditions for each element are summarized in Appendix 1.

Measurement of Se in the sediment

Selenium was measured by wet ashing and fluorometric detection based on Bayfield and Romalis (1985). Briefly, 50 mg of sample and 250 µL of standard solution were placed in a conical flask and combined with 3 mL of decomposition reagent (2:1 HNO_3:$HClO_4$). The mixture was heated at 130°C and raised to 190°C until digestion finished and the volume decreased. The flask was cooled, then 0.4 mL 5 N HCl was added, and the solution was heated at 130 to 150°C for 15 mins to reduce Se(VI) to Se(IV). After cooling, 2 mL of masking reagent (EDTA + hydroxylamine hydrochloride + 0.05% methyl orange) were added to bind interfering metals. 7.5 N NH_4OH was added dropwise until the solution became yellow, followed by 1 N HCl until a pink color appeared at pH 3. The solution was transferred to a test tube and diluted to 9 mL with milli-Q water. 1 mL of freshly prepared 2,3-diaminonaphthalene reagent was added, and the pH was set to 1.8. Tubes were covered with aluminum foil and incubated at 50°C for 30 minutes, then cooled. 5 mL of cyclohexane were added, and the mixture was shaken at 50 strokes per minute for 30 mins and centrifuged at 2000 rpm for 5 mins. The upper cyclohexane phase containing piazselenol was collected and analyzed with a fluorescence spectrophotometer (Hitachi F-2700 (Japan) Fluorescence Spectrophotometer). The excitation wavelength was set at 380.0 nm, and the emission wavelength was set at 525.0 nm, following the instrument's operating conditions.

Risk assessments

Sediment contamination was assessed using sediment quality guidelines (SQGs), consistent with the framework of MacDonald et al. (2000), including effect range-low (ERL) and effect range-median (ERM; Long et al., 1995), lowest effect level (LEL) and severe effect level (SEL; Persaud et al., 1993), threshold effect level (TEL) and probable effect level (PEL; Smith, 1996), and threshold effect concentration (TEC) and probable effect concentration (PEC; MacDonald et al., 2000). These SQGs were used to evaluate the potential biological relevance of metal concentrations in sediment samples, excluding Se and Sn due to the absence of established SQGs for these metals.

Contamination factors (CF) were calculated as the ratio of measured concentrations to natural background shale values (Turekian and Wedepohl, 1961; Zn = 95 mg kg^{-1}, Cu = 45 mg kg^{-1}, Cd = 0.3 mg kg^{-1}, Pb = 20 mg kg^{-1}, Se = 0.6 mg kg^{-1}, and Sn = 6 mg kg^{-1}) following Hakanson (1980), with CF less than 1 (low contamination), 1 to 3 (moderate contamination), 3 to 6 (considerable contamination), and greater than 6 (high contamination). The geoaccumulation index (I_{geo}) was computed using $\log_2$ of the measured concentrations and divided by the natural background shale values of each metal (Turekian and Wedepohl, 1961), and a correction factor of 1.5 following Müller (1979), with classes ranging from non-polluted (Igeo < 1) to very highly polluted (Igeo > 5). The pollution load index (PLI) was determined as the geometric mean of CF values across metals for each site following Tomlinson et al. (1980), with PLI > 1 indicating unpolluted conditions (Gopal et al., 2023).

Quality assurance/quality control (QA/QC)

Procedural blanks analyzed in five replicates quantified background contamination and instrument noise. Multi-point external calibration curves were produced for each analyte, and correlation coefficients exceeded 0.98. All samples for metal analysis were prepared and analyzed in duplicate, and method precision based on relative percent difference remained below 25%. Calibration standards at 0, 0.01, 0.1, 1, and 5 ppm were prepared by serial dilution of certified 1000 ppm stocks using 1% HNO_3, 3 M HCl, or 0.1 N HNO_3 depending on the analyte. Metal matrix spike recoveries ranged from 90% to 110%. Limits of detection and limits of quantification were computed from five blank readings and the slope of each calibration curve for all metals.

Data analysis

Descriptive statistics were reported as means and standard deviations when applicable. Correlation between sediment properties, metal bioavailable concentrations, and other measured variables were examined using Pearson correlation at p = 0.05 Correlation results were visualized using correlation matrices to aid interpretation of the strength and direction of associations. Principal component analysis (PCA) was performed in R Studio to examine metal relationships with sediment characteristics. All statistical analyses were completed using IBM SPSS, R Studio, and Microsoft Excel.

Results

Sediment characteristics

Sediment characteristics are shown in Table 1. Stations (Stations 5 and 6) relatively far away from the beach or shore and near coastal structures (Station 7) were found with higher moisture content and coincided with higher silt/clay fractions and higher total organic matter, while stations (Stations 2 and 4) close to the shore or beach, especially the seaweed farm stations (8, 9, and 10), and near residential areas were found with lower moisture content and aligned

with higher sand content. Moisture content showed a strong significant positive correlation with silt and clay ($r = 0.90$, $p < 0.05$) and total organic matter ($r = 0.94$, $p < 0.05$), while it exhibited a strong significant negative correlation with sand ($r = -0.88$, $p < 0.05$). It also showed a moderate significant negative correlation with redox potential ($r = -0.51$, $p < 0.05$). Sand significantly correlated strongly and negatively with silt and clay ($r = -0.99$, $p < 0.05$) and with total organic matter ($r = -0.87$, $p < 0.05$). Redox potential in all stations was positive (oxic) and showed moderate significant negative correlations with silt and clay ($r = -0.59$, $p < 0.05$) and with total organic matter ($r = -0.45$, $p < 0.05$). Silt and clay significantly correlated strongly with total organic matter ($r = 0.94$, $p < 0.05$). These results indicate a sediment matrix that varies predictably as grain size shifts across sites.

Table 1
Sediment characteristics across the sampling stations

Station	Moisture (%)	Redox (mV)	Sand fraction (%)						Silt/clay fraction (%)	Total organic matter (%)
			Very coarse sand	Coarse sand	Medium sand	Fine sand	Very fine sand	Total		
1	29.46 ± 5.53	293 ± 48.77	6.05 ± 3.61	3.40 ± 0.11	8.34 ± 0.07	9.89 ± 0.40	31.65 ± 2.41	59.33	40.65 ± 3.76	7.51 ± 0.48
2	27.64 ± 1.35	234.67 ± 24.50	3.39 ± 2.44	17.95 ± 13.66	52.33 ± 9.58	19.19 ± 4.52	6.40 ± 5.70	99.26	0.74 ± 0.52	4.73 ± 0.04
3	39.41 ± 5.05	166.33 ± 55.37	2.38 ± 1.77	2.12 ± 1.73	3.49 ± 2.94	1.76 ± 0.30	12.09 ± 1.23	21.84	78.08 ± 1.86	11.36 ± 5.42
4	30.40 ± 0.78	478.67 ± 43.53	7.60 ± 2.10	24.07 ± 2.01	57.63 ± 6.42	9.35 ± 2.76	1.12 ± 0.59	99.77	0.23 ± 0.12	7.75 ± 2.21
5	50.29 ± 1.25	154.67 ± 32.72	2.19 ± 1.20	1.26 ± 0.09	2.70 ± 0.10	1.92 ± 0.04	15.31 ± 0.09	23.38	77.05 ± 2.18	15.84 ± 1.77
6	52.39 ± 2.78	157.33 ± 77.94	0.92 ± 0.21	0.54 ± 0.02	0.74 ± 0.04	0.50 ± 0.03	8.30 ± 0.34	10.99	88.94 ± 0.41	17.78 ± 0.48
7	55.26 ± 1.50	129 ± 49.76	0.85 ± 0.28	0.65 ± 0.15	0.80 ± 0.01	0.36 ± 0.01	5.97 ± 0.34	8.64	91.35 ± 0.54	17.62 ± 2.54
8	28.57 ± 1.14	567 ± 23.46	23.13 ± 4.23	22.41 ± 4.37	38.59 ± 7.38	12.65 ± 3.70	2.98 ± 2.23	99.62	0.24 ± 0.17	5.89 ± 0.71
9	30.27 ± 1.37	555 ± 20.23	14.41 ± 9.38	20.44 ± 4.01	42.52 ± 5.88	12.73 ± 4.21	9.70 ± 5.00	99.39	0.20 ± 0.11	6.41 ± 1.19
10	20.48 ± 1.41	534 ± 8.89	46.52 ± 9.74	32.46 ± 7.39	14.32 ± 8.86	4.94 ± 2.68	1.35 ± 1.19	99.42	0.41 ± 0.08	4.21 ± 0.89

Values are presented as mean ± SD; *n = 3*

Spatial distribution

Spatial differences in Zn, Cu, Cd, Pb, Se, and Sn in sediments from September 2024 are shown in Fig. 2 and Fig. 3. Higher metal levels occurred at stations with higher silt/clay, higher moisture, and higher total organic matter. Stations 5, 6, and 7 met these conditions and recorded higher concentrations (Zn = 12.1–15.2 mg kg^{-1}; Cu = 2.37–3.28 mg kg^{-1}; Cd = 0.0518–0.0625 mg kg^{-1}; Pb = 2.70-3.00 mg kg^{-1}; Se = 6.24–7.31 mg kg^{-1}; Sn = 2.46–3.62 mg kg^{-1}) relative to other stations. Generally, metal concentrations increased with distance from the shoreline, whereas Se and inorganic Sn decreased.

Temporal variation of metals

In Fig. 4, monthly changes in sediment metals from September to November 2024 are shown. Zn and Se declined through time. In contrast, Cu, Cd, Pb, and Sn varied by month and station, with higher concentrations in September (Cu = 0.258–2.22 mg kg^{-1}; Cd = 0.0595–0.0718 mg kg^{-1}; Pb = 0.569–1.44 mg kg^{-1}; Sn = 2.29–2.62 mg kg^{-1}) and lower levels (Cu = 0.450 mg kg^{-1}; Cd = 0.0595 mg kg^{-1}) in the following months, although Pb (0.869 mg kg^{-1}) and Sn (4.45 mg kg^{-1}) peaked in November at Station 10.

Relationship of Zn, Cu, Cd, Pb, Se, Sn with sediment characteristics

Fifteen sediment and metal variables were reduced to four principal components explaining 89.76% of the total variance (Table S2). The data were suitable for PCA, with a Kaiser Meyer Olkin (KMO) value of 0.648 and a significant Bartlett's test ($p < 0.05$). PC1 explained 49.338% of the variance and showed strong positive loadings of silt and clay, moisture, total organic matter, and the bioavailable fractions of Pb, Zn, and Cu, while coarse and medium sand had strong negative loadings (Fig. 5). This indicates that fine textured, organic rich sediments control higher bioavailable metal levels. PC2 accounted for 21.728% of the variance and reflected differences in redox potential and sand content (Fig. 5). PC3 explained 10.576% of the variance and grouped very fine sand with Sn, Se, and Cd, indicating a distinct association. PC4 explained 8.117% of the variance and showed moderate loadings of fine sand with Zn and Cu. Correlation analysis supported these patterns, with strong positive correlations among bioavailable Zn, Cu, and Pb ($r = 0.92$ to 0.96, $p < 0.001$). Cu and Sn showed a weaker negative correlation ($r = -0.37$, $p < 0.05$), while Cd was negatively correlated with Sn ($r = -0.61$, $p < 0.001$). Overall, sediment texture and organic matter were the dominant controls on bioavailable metal distribution, while redox conditions and specific grain size fractions contributed secondary structure.

Risk assessment of measured bioavailable Zn, Cu, Cd, Pb, Se, and Sn

Measured sediment metal concentrations were compared with published sediment quality guidelines. Zn (2.26–15.2 mg kg^{-1}), Cu (0.26–3.28 mg kg^{-1}), Cd (0.05–0.07 mg kg^{-1}), and Pb (0.27-3.0 mg kg^{-1}) remained well below ERL (150 mg kg^{-1}), LEL (120 mg kg^{-1}), TEL (123 mg kg^{-1}), and TEC (121 mg kg^{-1}) thresholds, indicative of minimal ecological risk for these metals. Cd occurred at very low levels. Pb was consistently low. In contrast, Se ranged from 3.32 to 14.26 mg kg^{-1} and exceeded observed threshold values (threshold based on predicted effects = 2.5 mg kg^{-1}; observed threshold = 4 mg kg^{-1}; Van Derveer and Canton, 1997; Lemly, 1999) at several stations, which suggests potential for bioaccumulation despite the absence of high-tier benchmarks. Inorganic Sn ranged from 1.12 to 4.61 mg kg^{-1} but cannot be evaluated against guideline values, since none exist for bulk Sn, and toxicity assessment relies on organotin speciation. In these comparisons, the sediments showed low multi-metal pollution except for marked Se enrichment.

Risk assessment in sediment (CF, I_{geo}, and PLI) provides spatial and temporal context. Zn, Cu, Cd, Pb, and Sn showed CF values below 1 at all stations, which indicates low contamination. Selenium showed CF values from 6.45 to 23.8 across stations and months, which indicates very high contamination. Values were highest at Station 9 in September and declined toward November, although CF values in November still indicated considerable contamination. Geoaccumulation index (I_{geo}) values showed that Zn, Cu, Cd, Pb, and Sn fell within the non-polluted class (< 1) at all stations and months, while Se consistently showed positive I_{geo} values that corresponded to slight ($2 < I_{geo} < 3$) to moderate ($3 < I_{geo} < 4$) pollution. The highest Se enrichment occurred at Station 9 in September and at Station 8 in

October. Pollution load indices (PLI) further supported these findings. PLI values ranged from 0.107 to 0.343 across stations and months, and all were below the pollution threshold, which indicates that cumulative metal loading remained low despite the dominant contribution of Se to the CF and I_{geo} calculations.

Discussion

Sediment characteristics within and outside the seaweed farm

The texture of sediment indicates the dominant hydrodynamic energy. Sandy substrates prevail in high-energy nearshore areas, while silt/clay concentrates offshore under conditions of reduced wave and current activity. Coarse particles settle quickly, but fine sediments stay suspended and are carried seaward, resulting in an offshore fining trend (Ouillon, 2018). Fine sediments retain higher metal concentrations due to larger reactive surfaces, stronger organic matter associations, and reduced permeability that restricts porewater flow and favors long-term retention (Tavakoly Sany et al., 2013; Özşeker et al., 2022). It also shows strong coupling between moisture, total organic matter, and silt/clay fractions. Fine sediments retain water through cohesive forces and abundant sorption sites, promoting organic matter stabilization and longer solute residence times (Wang et al., 2011). Sandy sediments exhibit contrasting behavior precisely due to their higher permeability and restricted adsorption capacity (Hossain et al., 2014). Redox patterns follow texture, with fine sediments tending toward lower redox conditions due to enhanced organic matter degradation and surface-mediated reactions, while sandy layers remain more oxidizing through efficient oxygen exchange (Boguta et al., 2022).

Spatial distribution of metals

The spatial patterns of Zn, Cu, Cd, Pb, Se, and Sn (Fig. 2) depend on sediment conditions and local hydrodynamics. Fine sediment stations, especially 5, 6, and 7, showed the highest metal levels. Station 6 had 88.94% silt and clay, high moisture, elevated organic matter, and oxic redox conditions (Table 1). This station recorded the highest Zn and Cu and among the highest for Pb. Fine particles provide a large surface area and reactive sites for metal sorption, while organic matter forms stable complexes that strengthen retention (Tavakoly Sany et al., 2013). Sandy stations 2, 8, and 10 contained more than 99% sand and low organic matter. These stations had the lowest Zn, Cu, and Pb because coarse grains have large pore spaces, fast interstitial flow, and limited binding sites that favor particle flushing and reduce metal storage (Hossain et al., 2014). Cd and Se showed weaker spatial gradients. Cd stayed uniformly low and showed weak affinity to the dominant sediment matrix. Selenium remained even across the area with a localized rise at Station 9, a sandy site within the farm, which may indicate short-term depositional focusing or transient trapping linked to redox micro-conditions and particulate transport (Presser and Luoma, 2010). Inorganic Sn declined from Station 1 toward the interior of the farm, consistent with diffuse input near the power plant. Concentrations remained low, yet the persistence of Se and inorganic Sn warrants attention due to their potential for long-term buildup in sediments and biota.

Temporal variation of metals

Consistent temporal shifts were observed in bioavailable Zn, Cu, Cd, Pb, Se, and Sn concentrations in farm sediments from September to November 2024, with most metals showing higher concentrations in September followed by a general decline toward November. This pattern likely reflects post-monsoonal stabilization of sediments, reduced resuspension, and progressive consolidation of fine particles within the farm. Station 9 consistently recorded the highest bioavailable sediment concentrations, indicating localized enrichment linked to site-specific hydrodynamic conditions and proximity to potential sources. Zn showed the strongest decrease, from 13.14 mg kg^{-1} in September to 2.26 mg kg^{-1} in November, consistent with reduced particle mobilization and burial under calmer conditions (Birch,

2017). Cu followed a similar trend, reflecting its strong affinity for fine-grained sediments and organic matter under oxic conditions (Förstner and Wittmann, 2012). Cd remained relatively stable, ranging from 0.0455 to 0.0718 mg kg^{-1}, suggesting control by sediment composition rather than short-term redox changes (Luoma and Rainbow, 2008). Pb exhibited limited temporal variability and low concentrations, consistent with strong binding to sediment matrix that restrict mobility (Taylor and McLennan, 2001). Se showed the clearest seasonal response, declining from September to November at Stations 8 and 9 within a range of 3.32 to 14.26 mg kg^{-1}, consistent with its association with organic matter and redistribution as fine particle inputs decreased (Lemly, 1999). Inorganic Sn displayed the greatest spatial variability, particularly at Stations 9 and 10, with concentrations from 1.12 to 4.61 mg kg^{-1}, exceeding many coastal values (Hamed et al., 2013) and indicating localized inputs near the power plant followed by attenuation with distance.

PCA and correlation of sediment profiles and analyte concentrations

PC1 captured the dominant textural and geochemical gradient (Fig. 5). Sites with high silt/clay, high moisture, and high organic matter also had high Pb, Zn, and Cu. Sites with coarse to medium sand sat on the opposite end of the axis. This pattern fits known particle reactivity dynamics. Fine particles and organic matter offer high surface area and functional groups that bind divalent metals, which increases retention and lowers mobility (Eggleton and Thomas, 2004). The strong correlations among Pb, Zn, and Cu indicate similar depositional or anthropogenic inputs. Several urban and mariculture settings report the same grouping, often linked to industrial inputs and terrigenous material transported in suspension (Huang et al., 2019; Birch, 2017). The association with more reducing, cohesive silt/clay also matches observations that relatively low redox and high organic matter favor metal preservation in organic complexes (Di Toro et al., 1990). PC2 separated redox and larger sand fractions from very fine sand (Fig. 5). The result suggests that hydrodynamic sorting and oxygen supply vary together. Oxygenated sandy substrates tend to support nitrification and lower organic enrichment, while very fine sand accumulates in quieter zones with lower redox (Middelburg and Levin, 2009). PC3 grouped very fine sand, Sn, Se, and Cd. This association points to a distinct source or mineralogical control (Table S2). Cd often associates with carbonate or biogenic particles in coastal zones (Billah et al., 2019), while Se show affinity for fine aluminosilicates and oxyhydroxides under relatively suboxic conditions (Perkins and Foster, 2004). The grouping indicates that these three elements respond less to bulk organic gradients and more to specific grain size and diagenetic pathways. PC4 showed moderate loadings for fine sand with Zn and Cu, which suggests local textural modulation of metal concentrations independent of the main silt-organic gradient (Table S2). Together, the PCA and the pairwise correlations support three structural features in these sediments. First, fine cohesive substrates with higher organic matter act as the main sink for Pb, Zn, and Cu. Second, redox and hydrodynamic energy impose a secondary gradient that separates coarse sands from finer material. Third, Sn, Se, and Cd show a separate association driven by very fine grain size and possible mineralogical or diagenetic inputs. These features match reports from other tropical coasts with mixed natural and anthropogenic forcing (Birch, 2017; Huang et al., 2019).

Ecological risk assessment of metals in sediments

Multiple sediment indices were applied to address distinct assessment objectives. SQGs were used to assess the likelihood of adverse biological effects, while CF and I_{geo} were used to describe relative enrichment relative to background values. PLI was applied to provide an integrated view of cumulative metal loading across stations. Although these indices are partly correlated, their combined use allows separation of potential biological effects to its surrounding environment, enrichment status, and overall contamination patterns. Across all stations, Zn, Cu, Cd, and Pb concentrations remain well below established SQG thresholds, a concentration range where biological effects

are considered unlikely (Long et al., 1995; Persaud et al., 1993; Smith et al., 1996; MacDonald et al., 2000). These values indicate low sediment contamination and limited potential for direct toxicity to benthic organisms. Strong sorption of these metals to fine particles and organic matter further limits porewater exposure, supporting the interpretation of low ecological risk under current conditions (Long et al., 1995; MacDonald et al., 2000). Selenium differs from the other elements assessed. Its environmental relevance is linked to accumulative exposure rather than direct sediment toxicity, which explains its exclusion from ERL and ERM frameworks (Long et al., 1995; Kwok et al., 2014). Sediment Se concentrations approach levels reported to be associated with biological effects through food web transfer (Canton and Van Derveer, 1997; Lemly, 1999). This distinction is important for interpreting risk, as sediment guideline compliance alone does not fully capture Se behavior or potential exposure pathways.

Contamination factor and I_{geo} values classify Zn, Cu, Cd, Pb, and inorganic Sn as low contamination and nonpolluted across stations, while Se falls within higher contamination classes despite pollution load index values remaining below unity. This pattern reflects metal-specific geochemical behavior rather than broad or cumulative metal enrichment (Birch, 2017). PLI values inside and outside the farm consistently indicate low overall metal pressure, with no evidence that farming activities increase combined metal contamination. Overall, sediments within the study area can be characterized as low-contamination environments, while Se warrants separate consideration due to its distinct accumulation pathways and assessment framework.

The results indicate that the *Kappaphycus* farm situated in sediment environment classified as relatively unpolluted and can be considered relatively safe for potential contamination with respect to the metals analyzed. For monitoring and management of seaweed farms, this implies that routine assessments must be done especially in seaweed farm areas with similar context from this study and should not rely solely on bulk pollution indices but should include metal-specific levels.

Conclusion

Sediments surrounding the *Kappaphycus* seaweed farm in Concepcion, Iloilo generally contained low concentrations of bioavailable Zn, Cu, Cd, Pb, and Sn, with values well below commonly applied sediment quality guideline thresholds and indices. These results indicate minimal ecological risk from these metals under present environmental conditions. In contrast, Se concentrations exceeded several reported threshold values and indices, suggesting potential relevance in sediment health and for trophic transfer and long-term ecological monitoring. Spatial patterns show that metal distribution is primarily controlled by sediment texture and organic matter, with higher concentrations associated with fine grained, organic rich sediments. Temporal changes during the cultivation cycle indicate that sediment stabilization following the farming cycle may influence bioavailable metal availability within the farm environment. Overall, the study provides data on bioavailable metals in sediments of a tropical seaweed farming area and demonstrates the importance of sediment characteristics in controlling metal distribution. These findings contribute to environmental monitoring of coastal mariculture systems and support management strategies aimed at maintaining the environmental safety of farmed seaweeds.

Declarations

Statements and Declarations

All authors have read, understood, and have complied as applicable with the statement on “Ethical responsibilities of Authors” as found in the Instructions for Authors.

Competing Interests: This work was supported by the UPV OVCRE Student's Theses Support Grant, project number SP24-12, and by the UP OIL COOPERATE Mobility Grant, grant number OILCOOP-2024-15. The funders had no role in study design, data collection, data analysis, interpretation, writing, or decisions regarding publication. The authors declare no other competing interests.

Funding sources: This work was supported by the University of the Philippines Visayas Office of the Vice Chancellor for Research and Extension (UPV OVCRE) Student's Theses Support Grant (project number: SP24-12) and the University of the Philippines Office of International Linkages (UP OIL) Continuous Operational and Outcomes-based Partnership for Excellence in Research and Academic Training Enhancement (COOPERATE) Mobility Grant (grant number: OILCOOP-2024-15).

CRediT authorship contribution statement

Reyland Alegroso: Writing – original draft, Visualization, Methodology, Investigation, Formal analysis, Conceptualization. **Nathaniel Añasco:** Writing – review and editing, Supervision, Resources, Methodology, Conceptualization, Data curation. **Mae Grace Nillos**: Writing – review and editing, Methodology, Conceptualization, Validation, Data curation. **Sheila Mae Santander-de Leon**: Writing – review and editing, Methodology, Conceptualization, Validation, Data curation. **Kazuki Imamura:** Methodology, Investigation, Formal analysis, Data curation. **Emiko Kokushi:** Resources, Conceptualization, Methodology, Supervision. **Seiichi Uno**: Resources, Conceptualization, Methodology, Supervision.

Data availability statement

Data will be made available on request.

References

1. [PSA] Philippine Statistics Authority. Fisheries Statistics of the Philippines, 2020–2022. (2023). Retrieved 14 January 2026, from https://psa.gov.ph/content/fisheries-situation-report-january-december-2022
2. Ask, E. I., Batibasaga, A., Zertuche-Gonzalez, J. A., & De San, M. (2003). Three decades of *Kappaphycus alvarezii* (Rhodophyta) introduction to non-endemic locations. In *Proc Int Seaweed Symp* (Vol. 17, pp. 49–57).
3. Barik, S. S., Singh, R. K., Tripathy, S., Farooq, S. H., & Prusty, P. (2022). Bioavailability of metals in coastal lagoon sediments and their influence on benthic foraminifera. *Science of The Total Environment*, *825*, 153986. https://doi.org/10.1016/j.scitotenv.2022.153986
4. Bayfield, R. F., & Romalis, L. F. (1985). pH control in the fluorometric assay for selenium with 2, 3-diaminonaphthalene. *Analytical biochemistry*, 144(2), 569–576. https://doi.org/10.1016/0003-2697(85)90155-1
5. Besada, V., Andrade, J. M., Schultze, F., & González, J. J. (2009). Heavy metals in edible seaweeds commercialised for human consumption. *Journal of Marine Systems*, *75*(1–2), 305–313. https://doi.org/10.1016/j.jmarsys.2008.10.01
6. Billah, M. M., Kokushi, E., & Uno, S. (2019). Distribution, geochemical speciation, and bioavailable potencies of cadmium, copper, lead, and zinc in sediments from urban coastal environment in Osaka Bay, Japan. *Water, Air, & Soil Pollution*, *230*(7), 157. https://doi.org/10.1007/s11270-019-4196-8
7. Birch, G. F. (2017). Determination of sediment metal background concentrations and enrichment in marine environments–a critical review. *Science of the total environment*, *580*, 813–831. https://doi.org/10.1016/j.scitotenv.2016.12.028

8. Boguta, P., Skic, K., Baran, A., & Szara-Bąk, M. (2022). The influence of the physicochemical properties of sediment on the content and ecotoxicity of trace elements in bottom sediments. *Chemosphere*, *287*, 132366. https://doi.org/10.1016/j.chemosphere.2021.132366
9. Canton, S. P., & Van Derveer, W. D. (1997). Selenium toxicity to aquatic life: An argument for sediment-based water quality criteria. *Environmental Toxicology and Chemistry*, *16*(6), 1255–1259. https://doi.org/10.1002/etc.5620160622
10. Cyriac, M., Gireeshkumar, T. R., Furtado, C. M., Fathin, K. F., Shameem, K., Shaik, A., & Balachandran, K. K. (2021). Distribution, contamination status and bioavailability of trace metals in surface sediments along the southwest coast of India. *Marine Pollution Bulletin*, *164*, 112042. https://doi.org/10.1016/j.marpolbul.2021.112042
11. Di Toro, D. M., Mahony, J. D., Hansen, D. J., Scott, K. J., Hicks, M. B., Mayr, S. M., & Redmond, M. S. (1990). Toxicity of cadmium in sediments: The role of acid volatile sulfide. *Environmental Toxicology and Chemistry: An International Journal*, *9*(12), 1487–1502. https://doi.org/10.1002/etc.5620091208
12. Eggleton, J., & Thomas, K. V. (2004). A review of factors affecting the release and bioavailability of contaminants during sediment disturbance events. *Environment international*, *30*(7), 973–980. https://doi.org/10.1016/j.envint.2004.03.001
13. El-Sharkawy, M., Alotaibi, M. O., Li, J., Du, D., & Mahmoud, E. (2025). Heavy metal pollution in coastal environments: Ecological implications and management strategies: A review. *Sustainability*, *17*(2), 701. https://doi.org/10.3390/su17020701
14. Förstner, U., & Wittmann, G. T. (2012). *Metal pollution in the aquatic environment*. Springer Science & Business Media. 2nd Edition, Springer-Verlag, Berlin.
15. Gangoso, S. J., Del Rosario, R. M., & Walag, A. M. P. (2022). The concentrations of selected heavy metals in the surface sediments in three locations of southern Philippines. *Asian Journal of Biological and Life Sciences*, *11*(2), 515. https://doi.org/10.5530/ajbls.2022.11.69
16. Gopal, V., Krishnamurthy, R. R., Vignesh, R., Nathan, C. S., Anshu, R., Kalaivanan, R., & Abioui, M. (2023). Assessment of heavy metal contamination in the surface sediments of the Vedaranyam coast, Southern India. *Regional Studies in Marine Science*, *65*, 103081. https://doi.org/10.1016/j.rsma.2023.103081
17. Hakanson, L. (1980). An ecological risk index for aquatic pollution control. A sedimentological approach. *Water research*, *14*(8), 975–1001. https://doi.org/10.1016/0043-1354(80)90143-8
18. Hamed, M. A., Mohamedein, L. I., El-Sawy, M. A., & El-Moselhy, K. M. (2013). Mercury and tin contents in water and sediments along the Mediterranean shoreline of Egypt. *Egyptian Journal of Aquatic Research*, *39*(2), 75–81. https://doi.org/10.1016/j.ejar.2013.06.001
19. Holme, N. A., & McIntyre, A. D. (1971). *Methods for the study of marine benthos*. IBP Handbook No, 16. Blackwell Sci. Publ., Oxford and Edinburgh. F. A. Davis, Philadelphia. 346 p. https://doi.org/10.4319/lo.1972.17.6.0968
20. Hossain, M. B., Marshall, D. J., & Venkatramanan, S. (2014). Sediment granulometry and organic matter content in the intertidal zone of the Sungai Brunei estuarine system, northwest coast of Borneo. *Carpathian journal of earth and environmental sciences*, *9*(2), 231–239.
21. Huang, X., Luo, D., Zhao, D., Li, N., Xiao, T., Liu, J., & Liu, G. (2019). Distribution, source and risk assessment of heavy metal (oid) s in water, sediments, and Corbicula Fluminea of Xijiang River, China. *International Journal of Environmental Research and Public Health*, *16*(10), 1823. https://doi.org/10.3390/ijerph16101823
22. Janz, D. M., DeForest, D. K., Brooks, M. L., Chapman, P. M., Gilron, G., Hoff, D., & Wayland, M. (2010). Selenium toxicity to aquatic organisms. *Ecological assessment of selenium in the aquatic environment*, *1*, 141–231. https://doi.org/10.1201/ebk1439826775-c6

23. Kwok, K. W., Batley, G. E., Wenning, R. J., Zhu, L., Vangheluwe, M., & Lee, S. (2014). Sediment quality guidelines: challenges and opportunities for improving sediment management. *Environmental Science and Pollution Research*, *21*(1), 17–27. https://doi.org/10.1007/s11356-013-1778-7
24. Langston, W. J. (2020). Endocrine disruption and altered sexual development in aquatic organisms: an invertebrate perspective. *Journal of the Marine Biological Association of the United Kingdom*, *100*(4), 495–515. https://doi.org/10.1017/s0025315420000533
25. Lemly, A. D. (1999). Selenium transport and bioaccumulation in aquatic ecosystems: a proposal for water quality criteria based on hydrological units. *Ecotoxicology and Environmental Safety*, *42*(2), 150–156. https://doi.org/10.1006/eesa.1998.1737
26. Lemly, D. A. (2009). Aquatic hazard of selenium pollution from coal mining. *Book Chapter In: In: Fosdyke, Gerald B. ed. Coal Mining: Research, Technology and Safety. 167–183. Chapter 6*. Nova Science Publishers, Inc. 17p.
27. Long, E. R., Macdonald, D. D., Smith, S. L., & Calder, F. D. (1995). Incidence of adverse biological effects within ranges of chemical concentrations in marine and estuarine sediments. *Environmental management*, *19*(1), 81–97. https://doi.org/10.1007/BF02472006
28. Luoma, S. N., & Rainbow, P. S. (2008). *Metal contamination in aquatic environments: science and lateral management* (Vol. 126). Cambridge: Cambridge university press. ISBN 978-0-521-86057-4
29. MacDonald, D. D., Ingersoll, C. G., & Berger, T. A. (2000). Development and evaluation of consensus-based sediment quality guidelines for freshwater ecosystems. *Archives of environmental contamination and toxicology*, *39*(1), 20–31. https://doi.org/10.1007/s002440010075
30. Mateo, J. P., Campbell, I., Cottier-Cook, E. J., Luhan, M. R. J., Ferriols, V. M. E. N., & Hurtado, A. Q. (2021). Understanding biosecurity: knowledge, attitudes and practices of seaweed farmers in the Philippines. *Journal of Applied Phycology*, 33, 997–1010. https://doi.org/10.1007/s10811-020-02352-5
31. Middelburg, J. J., & Levin, L. A. (2009). Coastal hypoxia and sediment biogeochemistry. *Biogeosciences*, *6*(7), 1273–1293. https://doi.org/10.5194/bg-6-1273-2009
32. Muller, G. (1979). Schwermetalle in den sedimenten des Rheins-Veranderungen seit. *Umschav*, *79*, 133–149. https://doi.org/10.1007/BF01153502
33. Naciongayo, J. J., & Santander-de Leon, S. M. (2024). Assessment of Benthic Macrofauna and Sediment Characteristics of Boracay Island, Philippines. *Sustainable Aquatic Research*, *3*(1), 58–76. https://doi.org/10.5281/zenodo.11046358
34. Ouillon, S. (2018). Why and how do we study sediment transport? Focus on coastal zones and ongoing methods. *Water*, *10*(4), 390. https://doi.org/10.3390/w10040390
35. Özşeker, K., Erüz, C., & Terzi, Y. (2022). Evaluation of toxic metals in different grain size fractions of sediments of the southeastern Black Sea. *Marine Pollution Bulletin*, *182*, 113959. https://doi.org/10.1016/j.marpolbul.2022.113959
36. Perkins, R. B., & Foster, A. L. (2004). Mineral affinities and distribution of selenium and other trace elements in black shale and phosphorite of the Phosphoria Formation. In *Handbook of Exploration and Environmental Geochemistry* (Vol. 8, pp. 251–295). Elsevier Science BV. https://doi.org/10.1016/s1874-2734(04)80012-3
37. Pereira, J. G., Raikar, S. S., Bhatti, A. G., Fatarpekar, P. G., & Nasnodkar, M. R. (2023). Metal bioavailability, bioaccumulation, and toxicity assessment through sediment and edible biota from intertidal regions of the Aghanashini Estuary, India. *Marine Environmental Research*, *191*, 106172. https://doi.org/10.1016/j.marenvres.2023.106172

38. Persaud, D. J. R. H. A., Jaagumagi, R., & Hayton, A. (1993). Guidelines for the protection and management of aquatic sediment quality in Ontario. Retrieved: atrium.lib.uoguelph.ca. ISBN 0-7778-9248-7
39. Presser, T. S., & Luoma, S. N. (2010). A methodology for ecosystem-scale modeling of selenium. *Integrated Environmental Assessment and Management*, *6*(4), 685–710. https://doi.org/10.1002/ieam.101
40. Rubio, C., Napoleone, G., Luis-González, G., Gutiérrez, A. J., González-Weller, D., Hardisson, A., & Revert, C. (2017). Metals in edible seaweed. *Chemosphere*, *173*, 572–579. https://doi.org/10.1016/j.chemosphere.2017.01.064
41. Shimod, K. P., Vineethkumar, V., Prasad, T. K., & Jayapal, G. (2022). Effect of urbanization on heavy metal contamination: a study on major townships of Kannur District in Kerala, India. *Bulletin of the National Research Centre*, *46*(1), 4. https://doi.org/10.1186/s42269-021-00691-y
42. Siddique, A. B., Al Helal, A. S., Patindol, T. A., Lumanao, D. M., Longatang, K. J. G., Rahman, M. A., & Shaibur, M. R. (2025). Assessment of Heavy Metal Contamination and Ecological Risk in Urban River Sediments: A Case Study from Leyte, Philippines. *Pollutants*, *5*(1), 7. https://doi.org/10.3390/pollutants5010007
43. Smith, S. L., MacDonald, D. D., Keenleyside, K. A., Ingersoll, C. G., & Field, L. J. (1996). A preliminary evaluation of sediment quality assessment values for freshwater ecosystems. *Journal of Great Lakes Research*, *22*(3), 624–638. https://doi.org/10.1016/S0380-1330(96)70985-1
44. Tavakoly Sany, S. B., Salleh, A., Rezayi, M., Saadati, N., Narimany, L., & Tehrani, G. M. (2013). Distribution and contamination of heavy metal in the coastal sediments of Port Klang, Selangor, Malaysia. *Water, Air, & Soil Pollution*, *224*(4), 1476. https://doi.org/10.1007/s11270-013-1476-6
45. Taylor, S. R., & McLennan, S. M. (2001). Chemical composition and element distribution in the Earth's crust. *Encyclopedia of physical science and technology*, *312*, 697–719. https://doi.org/10.1016/b0-12-227410-5/00097-1
46. Tomlinson, D. L., Wilson, J. G., Harris, C. R., & Jeffrey, D. W. (1980). Problems in the assessment of heavy-metal levels in estuaries and the formation of a pollution index. *Helgoländer meeresuntersuchungen*, *33*(1), 566–575. https://doi.org/10.1007/bf02414780
47. Turekian, K. K., & Wedepohl, K. H. (1961). Distribution of the elements in some major units of the earth's crust. *Geological society of America bulletin*, *72*(2), 175–192. https://doi.org/10.1130/0016-7606(1961)72[175:doteis]2.0.co;2
48. Uno, S., Kokushi, E., Kawano, M., McElroy, A. E., & Koyama, J. (2017). Toxic evaluations of sediments in Tokyo Bay, Japan, using Japanese medaka embryos. *Environmental Science and Pollution Research*, 24(36), 27702–27709. https://doi.org/10.1007/s11356-016-7581-5
49. Wang, W. W., Li, D. J., Zhou, J. L., & Gao, L. (2011). Nutrient dynamics in pore water of tidal marshes near the Yangtze Estuary and Hangzhou Bay, China. *Environmental Earth Sciences*, *63*(5), 1067–1077. https://doi.org/10.1007/s12665-010-0782-1

Figures

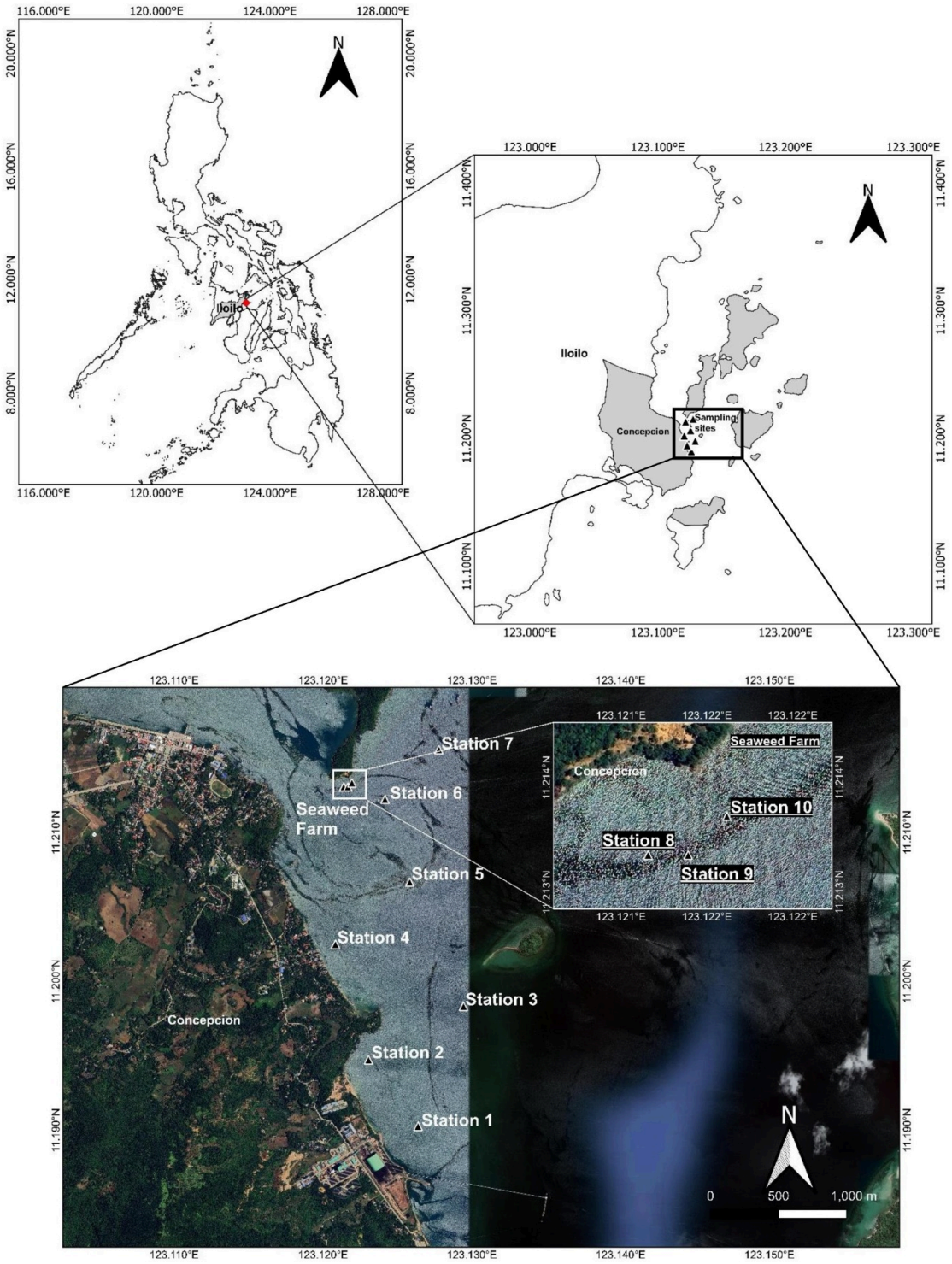
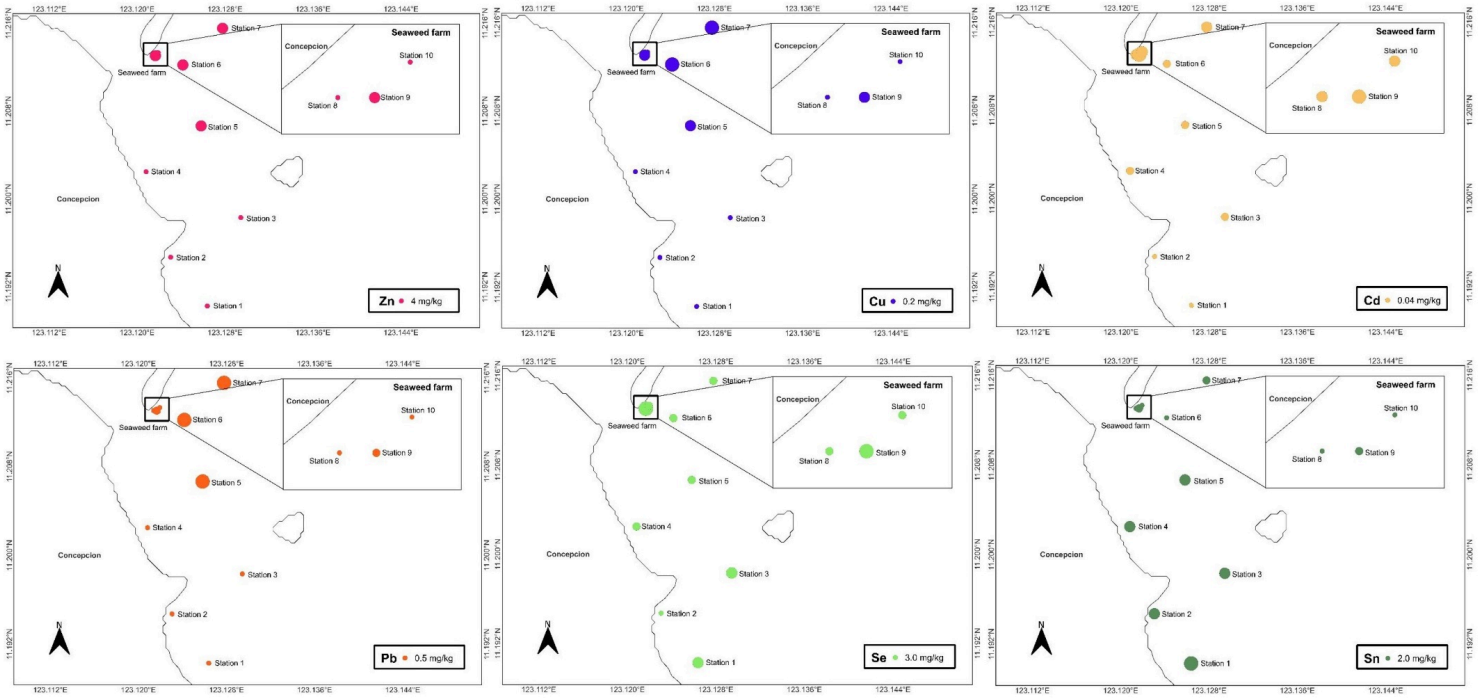


Figure 1: Study sampling map and sites in Concepcion, Iloilo, Philippines

Figure 1

Study sampling map and sites in Concepcion, Iloilo, Philippines, with triangular markers indicating the specific sampling coordinates

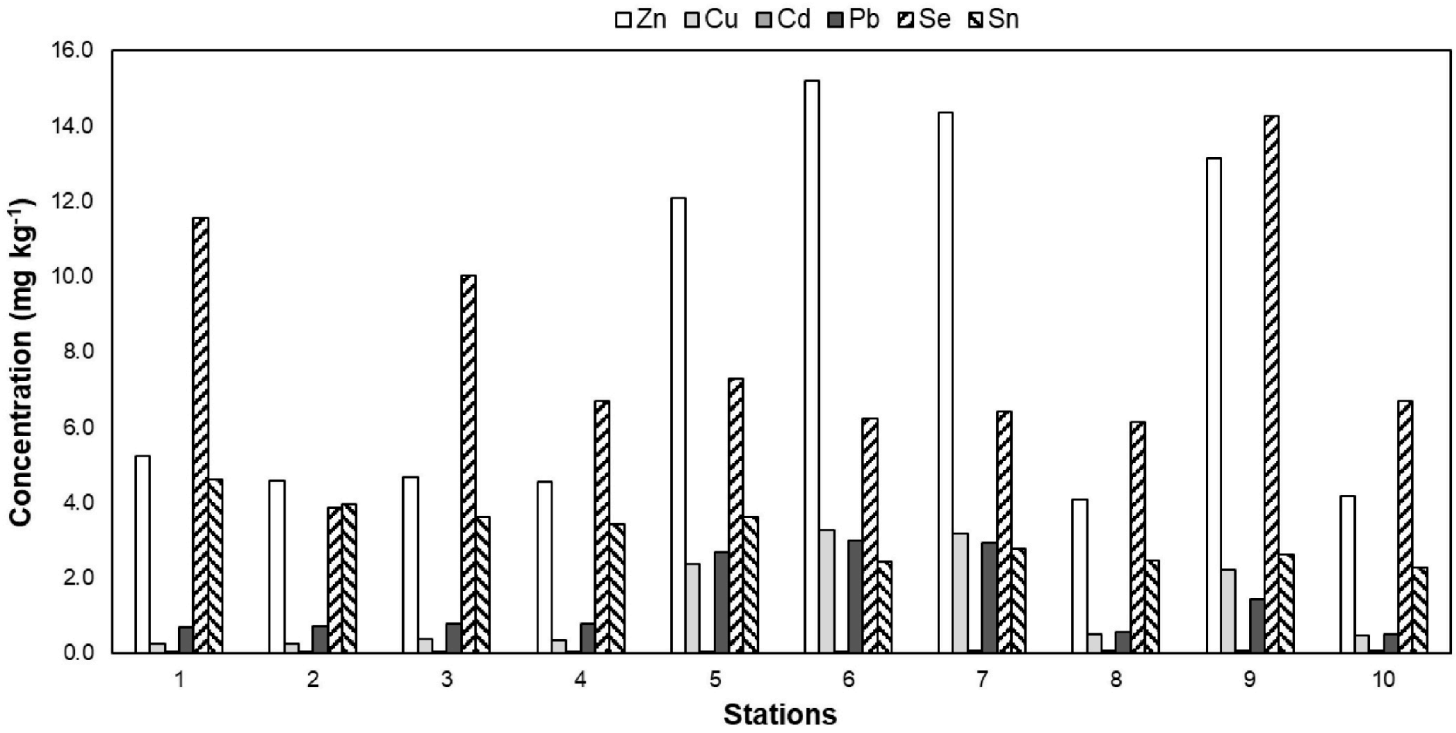


Values are presented as mean; *n = 2*. Concentrations are presented on a dry sediment weight basis.

Figure 2: Spatial distribution map of Zn, Cu, Cd, Pb, Se, and Sn in sediments within and surrounding the seaweed farm

Figure 2

Spatial distribution map of Zn, Cu, Cd, Pb, Se, and Sn in sediments within and surrounding the seaweed farm at specific coordinates

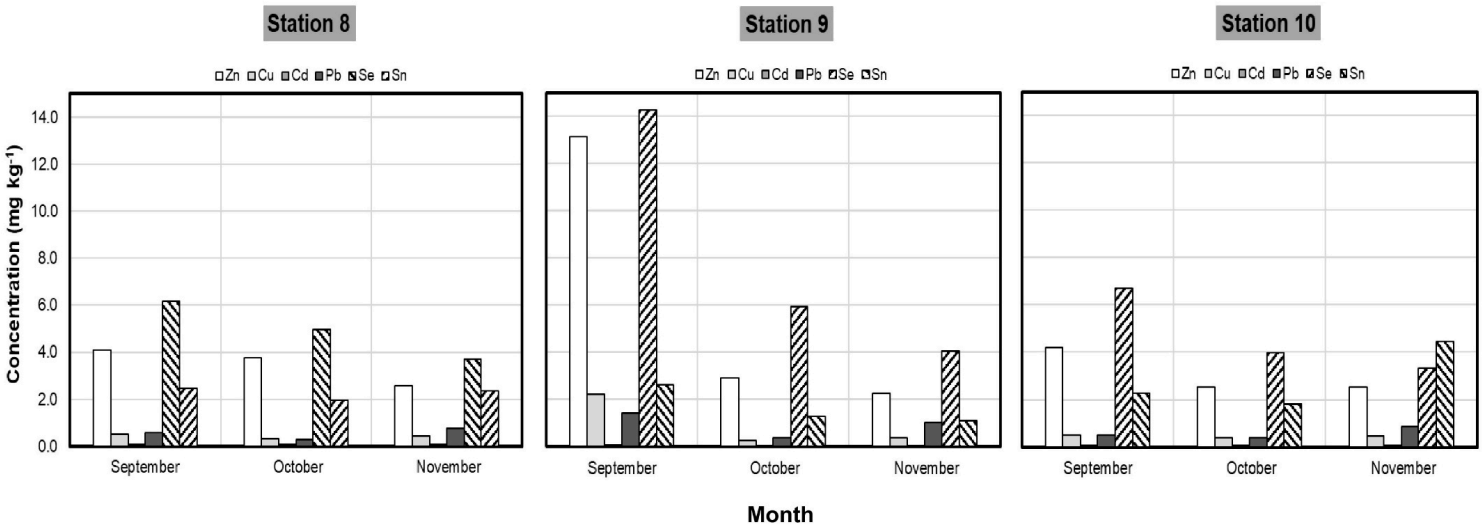


Values are presented as mean; *n = 2*. Concentrations are presented on dry sediment weight basis

Figure 3: Concentrations of Zn, Cu, Cd, Pb, Se, and Sn in sediments in different sampling stations collected in September 2024 *(n = 2)*

Figure 3

Concentrations of Zn, Cu, Cd, Pb, Se, and Sn in sediments in different sampling stations collected in September 2024 (*n = 2*)



Values are presented as mean; *n = 2*. Concentrations are presented on a sediment dry weight basis. Instrument detection limit (mg L^{-1}): Zn = 0.013; Cu = 0.0491; Cd = 0.00171; Pb = 0.0371; Se = 0.00718; Sn = 0.183.

Figure 4: Temporal variation of Zn, Cu, Cd, Pb, Se, and Sn concentrations in sediments from September to November 2025 across Stations 8, 9, and 10. Values are expressed in mg kg^{-1}.

Figure 4

Temporal variations of Zn, Cu, Cd, Pb, Se, and Sn concentrations in sediments from September to November 2025 across Stations 8, 9, and 10. Values are expressed in mg kg^{-1}

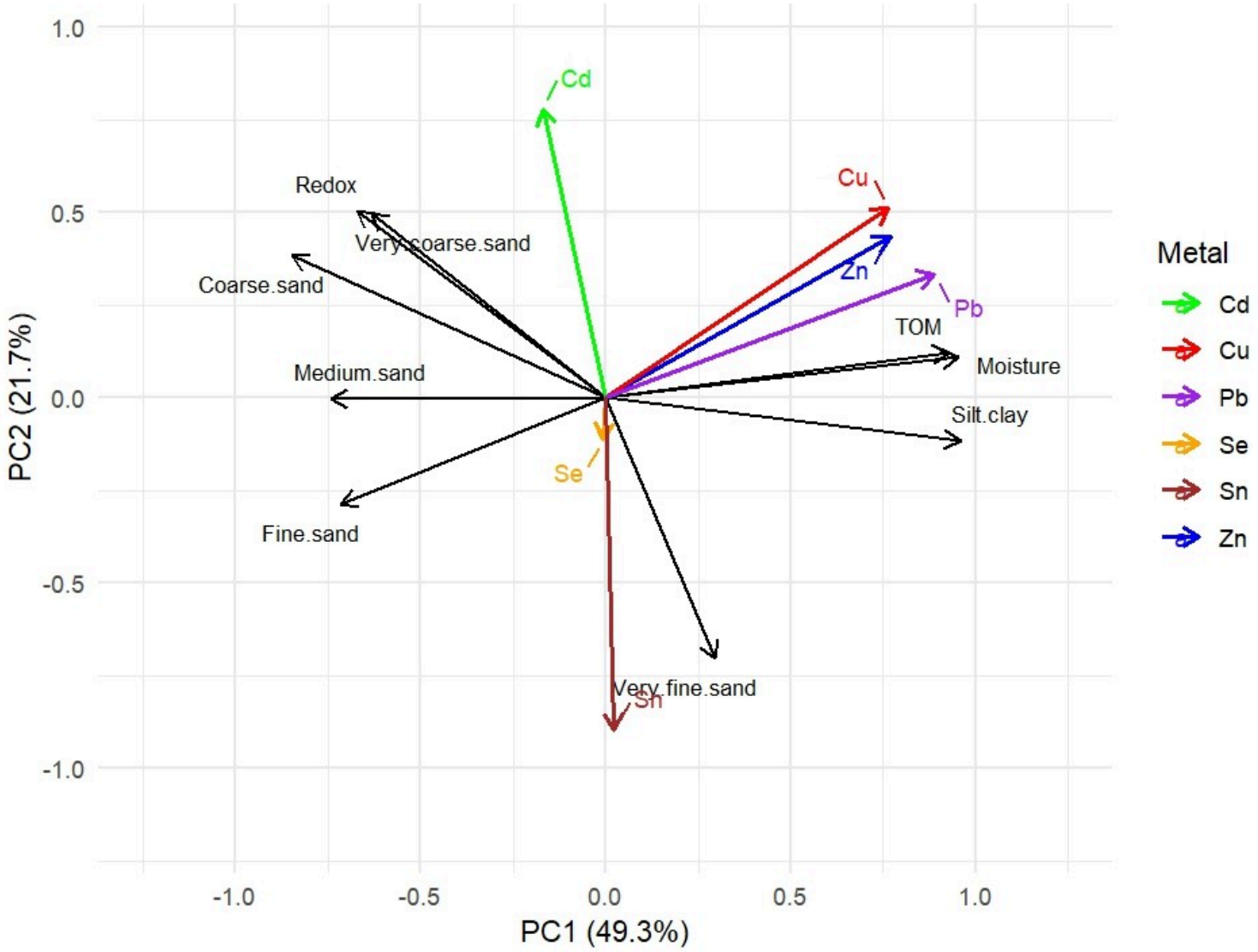


Figure 5

PCA biplot of PC1 (49.3%) and PC2 (21.7%) variances

Supplementary Files

This is a list of supplementary files associated with this preprint. Click to download.

- Appendices.docx